

AD-A103 908

CORNELL UNIV ITHACA NY DEPT OF MATERIALS SCIENCE AN--ETC F/G 11/2
AN AMORPHOUS ALLOY STRENGTHENED WITH A DISPERSION OF SECOND PHA--ETC(U)
AUG 81 H KIMURA, B CUNNINGHAM, D G AST
TR-6

N00014-77-C-0546

NI

UNCLASSIFIED

1-1
2-1



END

DATE

FILED

Q 81

DTIC

SECURITY CLASSIFICATION OF THIS PAGE (When Data Entered)

REPORT DOCUMENTATION PAGE		READ INSTRUCTIONS BEFORE COMPLETING FORM
1. REPORT NUMBER	2. GOVT ACCESSION NO.	3. RECIPIENT'S CATALOG NUMBER
4. TITLE (and Subtitle)	5. TYPE OF REPORT & PERIOD COVERED	6. PERFORMING ORG. REPORT NUMBER
7. AUTHOR(s)	8. CONTRACT OR GRANT NUMBER(s)	
9. PERFORMING ORGANIZATION NAME AND ADDRESS	10. PROGRAM ELEMENT, PROJECT, TASK AREA & WORK UNIT NUMBERS	
11. CONTROLLING OFFICE NAME AND ADDRESS	12. REPORT DATE	
14. MONITORING AGENCY NAME & ADDRESS (if different from Controlling Office)	13. NUMBER OF PAGES	
	15. SECURITY CLASS. (of this report)	
	15a. DECLASSIFICATION/DOWNGRADING SCHEDULE	
16. DISTRIBUTION STATEMENT (of this Report)		
17. DISTRIBUTION STATEMENT (of the abstract entered in Block 20, if different from Report)		
18. SUPPLEMENTARY NOTES		
19. KEY WORDS (Continue on reverse side if necessary and identify by block number)		
20. ABSTRACT (Continue on reverse side if necessary and identify by block number)		

AD A103908

DTIC FILE COPY

DD FORM 1 JAN 73 1473

EDITION OF 1 NOV 65 IS OBSOLETE
S/N 0102-LF-014-6601

SECURITY CLASSIFICATION OF THIS PAGE (When Data Entered)

DTIC
ELECTE
SEP 9 1981
A

81 9 06 92

403 152

AN AMORPHOUS ALLOY STRENGTHENED WITH A DISPERSION OF SECOND PHASE PARTICLES

H. KIMURA, B. CUNNINGHAM and D.G. AST

Materials Science and Engineering Department, Cornell University
Ithaca, New York 14853 U. S. A.

1. INTRODUCTION

Dispersion hardening is a well known mechanism to strengthen crystalline materials. Partial crystallization of amorphous alloys improves the yield strength (relative to the as-quenched alloy) but concomitantly the alloy tends to lose its ductility (1)(2)(3)(4).

This paper presents the first observation and measurement of the micro-structure and the mechanical properties of a ductile WC-particle containing amorphous alloy.

The present technique to prepare two-phase amorphous materials has the potential to improve properties such as strength, wear resistance and super-conductivity.

2. EXPERIMENTAL PROCEDURE

$\text{Ni}_{78}\text{Si}_{10}\text{B}_{12}$ was chosen because the amorphous alloy can be obtained easily at relatively low quenching rates (5) and has good ductility (6)(7). WC-particles were used as a hard second phase constituent since WC has a high Young's modulus of 68,000 kg/mm² (8). Both the non-dispersed, and the WC-containing alloys were prepared in a single drum quenching apparatus as continuous ribbon specimens of 40 μm thickness. The micro-structure of the WC-containing $\text{Ni}_{78}\text{Si}_{10}\text{B}_{12}$ was investigated by scanning electron microscopy and microprobe analysis (EDA) in a JEOL 733 as well as by transmission electron microscopy (TEM; JEOL CX200). Crystallization temperature was measured using a differential scanning calorimeter (DSC, Du Pont 990) at a heating rate of 50°C/minute.

Tensile yield stress was measured in an Instron testing machine at a cross-head-speed of 0.05 mm/min. Hardness was measured with a Knoop hardness tester under a load of 400 gr. Tensile fracture surface and deformation marking in bending were observed by scanning electron microscopy (SEM).

3. EXPERIMENTAL RESULTS

3-1. Transmission electron microscopy of the WC-containing amorphous alloy

Figure 1 shows (a) a dark field of the WC-containing $\text{Ni}_{78}\text{Si}_{10}\text{B}_{12}$ alloy, (b) a selected area electron diffraction pattern.

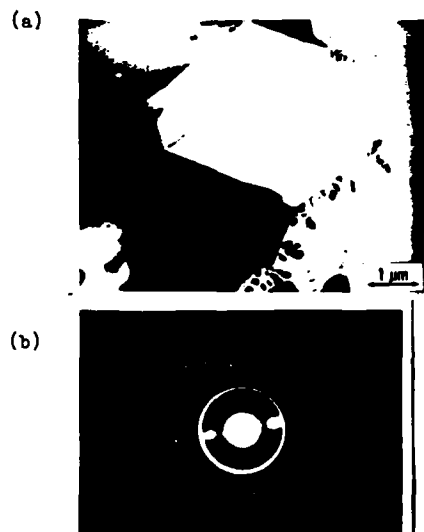


Fig. 1. Transmission electron micrographs of WC-containing amorphous $\text{Ni}_{78}\text{Si}_{10}\text{B}_{12}$: (a) a dark field $\vec{g} = (2\bar{2}01)$, and (b) the selected area diffraction pattern.

The micro-structure of the WC-containing $\text{Ni}_{78}\text{Si}_{10}\text{B}_{12}$ consists of an amorphous matrix and hexagonal-shaped WC-particles, 4-5 μm in size, containing some relative straight dislocations. The amorphous nature of the matrix is clearly indicated by halo patterns, and the h.c.p. structure of WC is easily identified by analyzing the diffraction pattern in Fig. 1(c). The dark field image was taken with the $(2\bar{2}10)$ reflection of WC.

A crystalline, metastable phase can occasionally be observed at the interface between the Ni_{78}

$\text{Si}_{10}\text{B}_{12}$ amorphous matrix and the WC-particles.

3-2. Distribution of WC-particles

Figure 2(a) shows the distribution of WC-particles on the specimen surface as revealed by compositional backscattering mode in the JEOL 733.

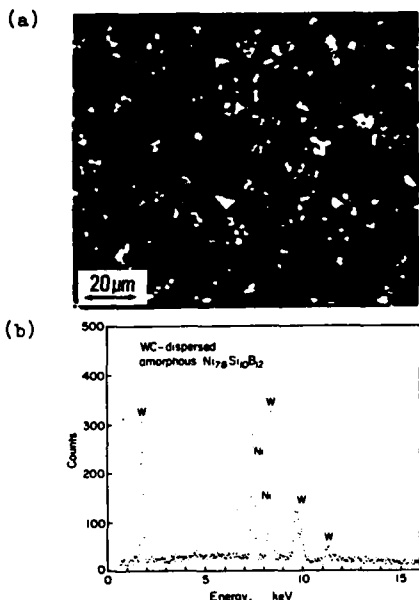


Fig. 2. Surface images of the WC-distributed amorphous $\text{Ni}_{78}\text{Si}_{10}\text{B}_{12}$ (a) compositional backscattering mode in the JEOL 733, (b) energy dispersive analysis spectrum of a bright particle.

The presence of WC, which is seen as white dots in Fig. 2(a), was confirmed by the EDA. Figure 2(b) shows that the X-ray spectrum of a particle with a white contrast contains the characteristic lines of tungsten. The WC-particles are uniformly distributed throughout the amorphous matrix. From Fig. 2(a), we estimate the WC-volume fraction of the dispersed amorphous alloy as about 7%.

3-3. Mechanical property of the WC-dispersed amorphous $\text{Ni}_{78}\text{Si}_{10}\text{B}_{12}$

3-3-1. Bending deformation

WC-dispersed amorphous $\text{Ni}_{78}\text{Si}_{10}\text{B}_{12}$ can be bent back 180° without fracturing. Figure 3 is (a) a secondary electron image and (b) a compositional image of the surface of a bent WC-dispersed alloy. We find that the slip bands by-pass the second phase particles or agglomerates. Such a delocalization of

the slip bands is expected to increase the strength of a dispersed amorphous alloy.

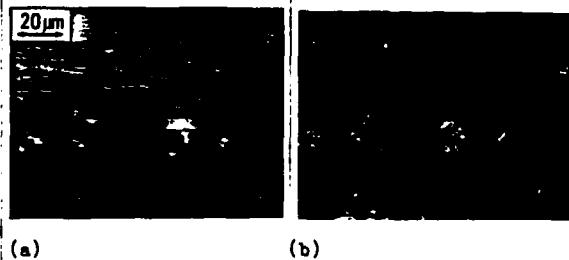


Fig. 3. Deformation marking of bent WC-dispersed amorphous $\text{Ni}_{78}\text{Si}_{10}\text{B}_{12}$ ribbons (a) a secondary electron image and (b) a compositional image.

3-3-2. Tensile Yield Stress

Figure 4 shows the tensile stress-extension curves for the WC-dispersed and non-dispersed amorphous $\text{Ni}_{78}\text{Si}_{10}\text{B}_{12}$.

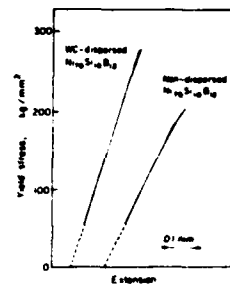


Fig. 4. Stress-extension curves for non-dispersed, and WC-dispersed amorphous $\text{Ni}_{78}\text{Si}_{10}\text{B}_{12}$.

Fig. 4 shows that specimens fractured within the elastic region, after some deviation from linearity in the stress-extension curves. The WC-dispersed amorphous $\text{Ni}_{78}\text{Si}_{10}\text{B}_{12}$ (7% WC-volume fraction) has a yield strength of 280 kg/mm²; this stress level is 1.4 times higher than that of 203 kg/mm² for non-dispersed amorphous $\text{Ni}_{78}\text{Si}_{10}\text{B}_{12}$. The presence of the vein pattern and a featureless slip zone on the tensile fracture surface indicates a shear slip process; i.e., the tearing mode (10) (11). For this reason, the fracture stress may represent the general yield stress of the thin specimen of WC-dispersed amorphous $\text{Ni}_{78}\text{Si}_{10}\text{B}_{12}$. The yield stress (203 kg/mm²) of non-dispersed amorphous $\text{Ni}_{78}\text{Si}_{10}\text{B}_{12}$ follows Hill's relation between hardness and shear stress of a rigid perfectly plastic material (6). Table 1 summarizes these results.

3-3-3. Fractography

Figure 5a is a secondary electron image and (b) a

Composition	WC-volume fraction, %	Yield stress kg/mm ²	Knoop hardness kg/mm ²	Young's modulus kg/mm ²	Crystallization temp, K
WC-Ni ₇₈ Si ₁₀ B ₁₂	7	280	—	12200 ^a	723
Ni ₇₈ Si ₁₀ B ₁₂	0	203	635	8000	717

^aestimated value based on eqn. 1

Table 1. Mechanical and thermal characteristics of WC-dispersed and non-dispersed amorphous Ni₇₈Si₁₀B₁₂.

compositional image of the same fracture surface of a WC-dispersed alloy. Fig. 5 indicates that fracture of a WC-dispersed amorphous alloy occurs by a slip process after plastic instability.

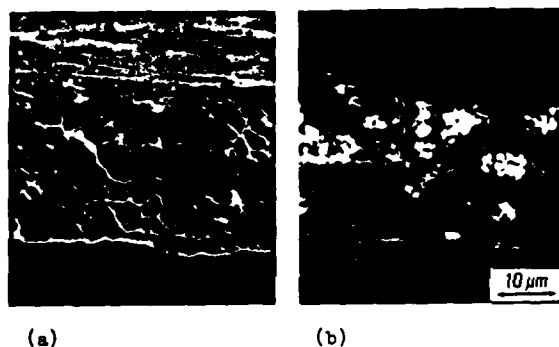


Fig. 5. Tensile fracture surface of the WC-dispersed amorphous Ni₇₈Si₁₀B₁₂ (a) a secondary electron image and (b) a compositional image.

Figure 6 shows a fracture surface with a high volume fraction of WC. A vein pattern is still observed in Fig. 6, indicating a ductile failure mode.

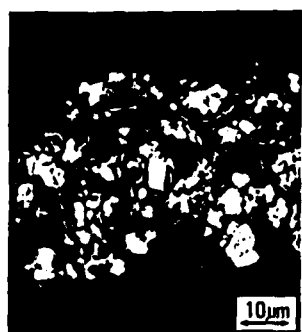


Fig. 6. A compositional image of fracture surface of the WC-dispersed amorphous Ni₇₈Si₁₀B₁₂.

In addition, both fracture surfaces of the WC-dispersed amorphous Ni₇₈Si₁₀B₁₂ show an identical distribution of WC particles on both surfaces.

This indicates that the WC-particles or agglomerates do not act as the initiation site for decohesion, but are load bearing in the soft matrix (liquid layer) of the slip band after plastic instability commences.

4. DISCUSSION

We provide two simple bounds on the Young's modulus for a composite (two phase material) (12). The upper bound, which assumes equal strain in both phases under elastic deformation is given by:

$$E = E_m (1 - V_f) + E_p V_f \quad (1)$$

where E is the effective modulus, E_m, and E_p are the Young's modulus of the matrix and second phase particle respectively, and V_f is the volume fraction of the second phase particles. The lower bound is:

$$E = \left(\frac{1 - V_f}{E_m} + \frac{V_f}{E_p} \right)^{-1} \quad (2)$$

which is based on an equal stress model.

Figure 7 shows the yield stress of the WC-dispersed Ni₇₈Si₁₀B₁₂ as a function of volume fraction.

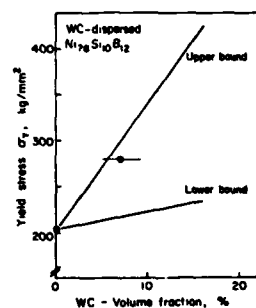


Fig. 7. Tensile yield stress of the WC-dispersed amorphous Ni₇₈Si₁₀B₁₂ as a function of volume fraction of WC.

The yield stress (σ_y) of various amorphous alloys correlates with Young's modulus: (13)

$$\sigma_y = E_m / \alpha \quad (3)$$

where α is a constant ranging from 30-40. If we apply Eqn. (3) to the yield stress of the WC-dispersed amorphous alloy, its yield stress (σ_{YWC}) is:

$$\sigma_{YWC} = E / \alpha \quad (4-a)$$

Substituting Eqn. (3) into Eqn. (4-a) yields:

$$\sigma_{YWC} = \sigma_Y \frac{E}{E_m} \quad (4-b)$$

Combining Eqn. (1) and (2) with Eqn. (4-b) respectively we get two expressions for dispersion hardening. The upper bound on the yield stress is:

$$\sigma_{YWC} = \sigma_Y \left\{ 1 + V_f \left(\frac{E_p}{E_m} \right) - 1 \right\} \quad (5)$$

The lower bound is:

$$\sigma_{YWC} = \sigma_Y \left\{ 1 + V_f \left(\frac{E_p}{E_m} \right) - 1 \right\}^{-1} \quad (6)$$

The solid lines in Fig. 7 denote prediction of Eqn. (5) and (6) using values of 68,000 kg/mm² and 8,000 kg/mm² for Young's modulus of WC and amorphous Ni₇₈Si₁₀B₁₂ respectively.

The yield stress of the WC-dispersed amorphous Ni₇₈Si₁₀B₁₂ appears to increase with volume fraction according to the upper bound rule of Eqn. (6). If Eqn. (6) indeed applies, a considerable improvement of the strength of the matrix material can be obtained with a small fraction of hard particles.

Further measurement of the yield stress and Young's modulus as a function of volume fraction are being carried out.

5. CONCLUSIONS

1. We have succeeded in preparing the WC-containing amorphous Ni₇₈Si₁₀B₁₂. This alloy has good ductility and can be bent back 180° without fracturing.

2. Transmission electron microscopy confirms that the Ni₇₈Si₁₀B₁₂ matrix is amorphous, and the WC hexagonal. SEM images indicate a uniform dispersion of WC-particles or particle agglomerates in the amorphous matrix.

3. The yield stress of the WC-dispersed amorphous Ni₇₈Si₁₀B₁₂ is 1.4 times higher than that of non-dispersed Ni₇₈Si₁₀B₁₂. The increase is the yield stress for the WC-dispersed amorphous alloy appears to obey the mixture rule (upper bound) for two phase materials.

4. The slip bands, as tested in bending, bypass WC-particles or particle agglomerates. Tensile fracture surface of the WC-dispersed alloy is composed of a "vein" pattern containing the WC-particle

and a featureless smooth zone.

ACKNOWLEDGEMENTS

The research was sponsored by the Office of Naval Research under Contract NR 039-151-N00014-77-C-0546 and supported by additional funds from the Materials Science Center at Cornell University.

We thank B. Addis for help in preparing the amorphous alloys.

REFERENCES

1. T. Masumoto and R. Maddin, *Acta Metall.*, 19, 725 (1971).
2. C.-P. Chou and F. Spaepen, *Acta Metall.*, 23, 609 (1975).
3. R.L. Freed and J.B. Vander Sande, *Acta Metall.*, 28, 103 (1980).
4. H. Kimura and T. Masumoto, *Acta Metall.*, 28, 1677 (1980).
5. T. Minemura, et. al., *The Meeting of Japan Inst. Metals*, Aug. (1976).
6. H. Kimura and T. Masumoto, *Phil. Mag.*, in press.
7. I.W. Donald and H.A. Davies, *Phil. Mag.*, 42, 277 (1980).
8. J.F. Lynch, et. al., "Engineering Properties of Selected Ceramic Materials," *Am. Ceram. Soc.* Columbus, Ohio, 1966.
9. H.J. Leamy, et. al., *Metall. Trans.*, 3, 699, (1972).
10. H. Kimura and T. Masumoto, *Scripta Metall.*, 9, 211 (1975).
11. H. Kimura and T. Masumoto, *Acta Metall.*, 28, 1663 (1980).
12. For example, L.J. Broutman and R.H. Krock, *Modern Composite Materials*, Addison-Wesley, Reading, Mass., 1967.
13. L.A. Davis, et. al., *Scripta Metall.*, 10, 937 (1976).

Accession For	<input checked="" type="checkbox"/> <input type="checkbox"/> <input type="checkbox"/>
DTIC GRA&I	
DTIC TAB	
Unannounced	
Justification	
By	
Distribution/	
Availability Codes	
Avail and/or	
Special	
A	